Effect of Deformation Schedule on the Microstructure and Mechanical Properties of a Thermomechanically Processed C-Mn-Si Transformation-Induced Plasticity Steel

I.B. TIMOKHINA, P.D. HODGSON, and E.V. PERELOMA

Thermomechanical processing simulations were performed using a hot-torsion machine, in order to develop a comprehensive understanding of the effect of severe deformation in the recrystallized and nonrecrystallized austenite regions on the microstructural evolution and mechanical properties of the 0.2 wt pct C-1.55 wt pct Mn-1.5 wt pct Si transformation-induced plasticity (TRIP) steel. The deformation schedule affected all constituents (polygonal ferrite, bainite in different morphologies, retained austenite, and martensite) of the multiphased TRIP steel microstructure. The complex relationships between the volume fraction of the retained austenite, the morphology and distribution of all phases present in the microstructure, and the mechanical properties of TRIP steel were revealed. The bainite morphology had a more pronounced effect on the mechanical behavior than the refinement of the microstructure. The improvement of the mechanical properties of TRIP steel was achieved by variation of the volume fraction of the retained austenite rather than the overall refinement of the microstructure.

I. INTRODUCTION

FROM the mid-1980s, attention has focused on enhancing the safety level of automobiles while reducing vehicle weight. One of the important factors contributing to the use of steel in the automotive industry is its higher strength and higher residual ductility at any given strength level.[1] Transformation-induced plasticity (TRIP) steels have been introduced as a fundamentally different type of higher-strength steel.[2,3] The microstructure of these steels, with a typical composition of Fe-0.2C-1.7Mn-1.5Si (in wt pct), consists of polygonal ferrite, bainite, martensite, and a significant amount of retained austenite.[4] The higher level of ductility is achieved by the transformation of metastable retained austenite to martensite during forming of the component at room temperature. The amount and stability of the retained austenite controls the mechanical properties of TRIP steels.[5] One of the most important factors that affects the mechanical and chemical stability of the retained austenite is the bainite morphology.[6,7,8] For example, acicular ferrite has been shown to result in a significant increase in the quantity and quality of the retained austenite, which then improved the room-temperature mechanical properties of TRIP steels.[8] The thermomechanical processing schedule can also affect the retained-austenite characteristics.

Traditionally, the main objective in conventional thermomechanical processing has been to refine the ferrite grain size through (1) refining the prior-austenite grains, (2) increasing the grain-boundary area per unit volume by changing the grain shape, *e.g.,* pancaking, and (3) increasing the density of intragranular defects (deformation bands and twin boundaries).[9] Moreover, it has also been observed that the volume fraction of retained austenite is related to the grain diameter of the polygonal ferrite; *i.e.,* the decrease in the polygonal ferrite grain diameter leads to the increase in the volume fraction of the retained austenite.[10] In steels with the presence of bainite in the microstructure, the other aim of thermomechanical processing is to refine the bainite by the deformation in the nonrecrystallized austenite region. It has been reported that the bainite can be significantly refined by more than 50 pct deformation in the nonrecrystallized region.[11] This can affect the mechanical and chemical stability of retained austenite present within bainite. Furthermore, the thermomechanical processing schedule also influences the transformation behavior, leading to different morphologies of the bainite.

The TRIP steels are typically produced on a hot-strip mill, where the level of roughing rolling (deformation in the recrystallized austenite region) and finishing rolling (deformation in the nonrecrystallized region) depend on the mill configuration and the starting and final thicknesses of the plates. It is possible to have accumulated finishing strains from 1 to over 2.5, where, for C-Mn-Si microalloyed steel, the strain in the finishing mill is accumulated. Prior to finishing, the austenite grain size will vary, depending upon the amount of reduction and the time between roughing and finishing. Hence, in the current work, a wide range of roughing and finishing strains were used to clarify the effect of different prior-austenite conditions on the transformation kinetics and mechanical properties of TRIP steels.

II. EXPERIMENTAL

The 0.2C-1.55Mn-1.55Si (in wt pct) steel was received as a hot-rolled plate from BHP Research-Melbourne Laboratories. The experiments were performed using a hot-torsion machine at a strain rate of 2.95 s^{-1} and rotation per second

I.B. TIMOKHINA, formerly Postdoctoral Student, School of Engineering and Technology, Deakin University, is Research Fellow, School of Physics and Materials Engineering, Monash University, VIC 3800, Australia. Contact e-mail: liana.timokhina@spme.monash.edu.au P.D. HODGSON, Professor, is with the School of Engineering and Technology, Deakin University. E.V. PERELOMA, Senior Lecturer, is with the School of Physics and Materials Engineering, Monash University, VIC 3800, Australia.

Manuscript submitted May 17, 2002.

of 4.86. Torsion allows higher amounts of deformation in the recrystallized and nonrecrystallized austenite regions compared with compression or laboratory rolling, which is critical for hot-strip mill simulation.[12] Torsion specimens with a gage length of 20 mm and diameter of 6.7 mm were machined from the plates, with the longitudinal axis parallel to the original rolling direction.

The processing schedule is shown in Figure 1. After austenitizing at 1250 °C for 120 seconds, the first sample was subjected to two deformations, with an equivalent tensile strain (ε) (hereafter called "strain") of $\varepsilon_1 = 0.25$ in the austenite recrystallization region and of $\varepsilon_2 = 0.47$ in the low-temperature nonrecrystallization region. After the second deformation, specimens were cooled at 1 Ks^{-1} to the accelerated-cooling start temperature (T_A) of 670 °C. This was followed by accelerated cooling at ~20 Ks^{-1} to 500 °C and then slow cooling at 5 Ks^{-1}, to avoid undershoot to the simulated coiling temperature of 450 °C. Samples were held for a 600 seconds to allow the isothermal bainitic transformation to take place and then were quenched to room temperature. The temperature of the samples was controlled by thermocouples inserted in 3 mm centerline holes in the grips at both ends of the sample.

To clarify the effect of heavy deformation (ε_1) in the recrystallized austenite region, various levels of deformation ($\varepsilon_1 = 0.25$, 0.5, and 0.75) were used with a range of strains in the nonrecrystallized austenite region (Table I). The effect of the deformation in the nonrecrystallized austenite region was studied by increasing the strain up to 3.0, with the deformation in the recrystallized austenite region increased gradually from 0.25 to 0.75 (Table I). The total strain also gradually increased from 0.72 to 3.75 (Table I). The accelerated-cooling start temperature was varied from

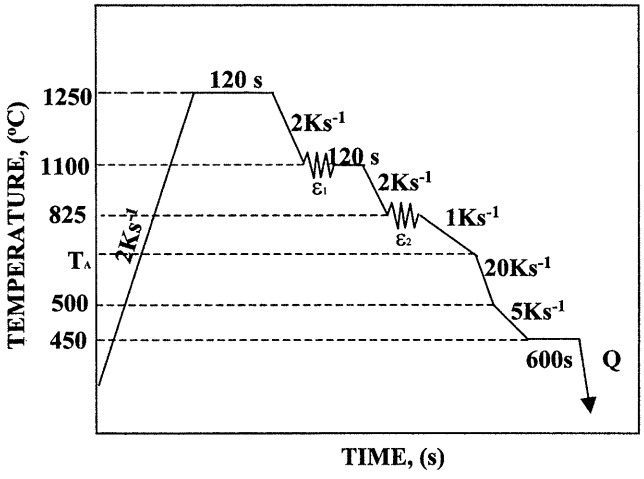

Fig. 1—Thermomechanical processing schedule.

Table I. Deformation Schedules

	Schedule					
Strain	1	2	3	4	5	6
ε_1	0.25	0.5	0.25	0.5	0.75	0.75
ε_2	0.47	0.47	1.2	1.2	1.2	3.0
$(\varepsilon_1 + \varepsilon_2)$	0.72	0.97	1.45	1.7	1.95	3.75

670 °C to 690 °C to maintain the polygonal ferrite content between 50 and 55 pct.

Specimen preparation for optical examination involved standard metallographic procedures. The samples were etched with 2 pct Nital to reveal the basic microstructure. For metallography, the torsion samples were sectioned along the longitudinal axis of the samples. All micrographs were taken near the surface of the samples. Selected samples were investigated using a field-emission scanning electron microscope (JEOL* JSM 630), operating at a 15 kV accelerating voltage.

*JEOL is a trademark of Japan Electron Optics Ltd., Tokyo.

Optical microscopy was supplemented by transmission electron microscopy (TEM) using a PHILIPS* CM20 micro-

*PHILIPS is a trademark of Philips Electronic Instruments Corp., Mahwah, NJ.

scope at an accelerating voltage of 200 kV. The foils for TEM were prepared by twin-jet polishing using a solution of 5 pct perchloric acid in methanol at −20 °C and an operating voltage of 60 V. The volume fraction of retained austenite was measured using a tint-etching technique. The color etchant was a mixture of three ingredients (4 pct HNO_3 + 7 pct $(NO_2)_3C_6H_2OH$ + saturated $Na_2S_2O_3$).[13] An X-ray diffraction analysis was carried out on the sample after $\varepsilon_1 = 0.25$ and $\varepsilon_2 = 0.47$, using a PHILIPS PW 1130 (40 kV, 30 mA) diffractometer equipped with a monochromator and Cu K_α radiation to confirm the results of the retained-austenite amount obtained after the tint etching. The retained-austenite volume fraction was calculated from the integrated intensities of $(200)_\alpha$, $(211)_\alpha$, $(200)_\gamma$, and $(220)_\gamma$. The prior-austenite grain size of quenched samples was revealed using a solution of 2 g picric acid and 0.5 g copper(II) chloride in 100 mL of water with 2 mL wetting agent. The quantitative analysis of retained austenite and the measurements of the prior-austenite grains were performed using UTHSCSA image-analysis software.

The microhardness of the second phase (bainite with retained austenite and martensite) was measured utilizing a Matsuzawa microhardness tester with a 25-g load. Room-temperature mechanical properties were determined using a shear-punch technique. This technique has been developed for cases when only a small amount of material is available. The in-house–manufactured rig was attached to an Instron 4500 tensile tester. A 5 kN load cell with a 0.25 mm/min crosshead speed and a 3-mm-diameter punch was used in the tests. The samples were taken from an outer annular section of the torsion specimens, cutting parallel to the torsion axis in the range of a 300 to 350 μm thickness. The test was instrumented to provide punch load-displacement data to determine tensile strength using the following empirical equation:[14]

$$\sigma_{\text{eff}} = \frac{P - F}{2\pi rt} = C\sigma \qquad [1]$$

where P is the maximum load (Newtons), σ is the corresponding uniaxial stress (mega Pascals), F is the friction load (Newtons), r is the punch radius (millimeters), t is the specimen thickness (millimeters), and C is an empirical correlation coefficient. From previous work,[15] the correlation

coefficient between the shear-punch load-displacement curves and uniaxial tensile data was determined to be $C = 0.58$.

The total elongation was calculated using an empirical equation:[14]

$$El_{\text{Total}} = \frac{d_f}{t} \quad [2]$$

where El_{Total} is the total elongation and d_f is the displacement at failure.

III. RESULTS

A. *Effect of Deformation in the Recrystallized Austenite Region on the Microstructure and Mechanical Properties of TRIP Steel*

The volume fraction and stability of the retained austenite determine the mechanical properties of the TRIP steels. The two metallurgical processes (ferrite transformation and bainite transformation) are important for the retained-austenite stabilization. The volume fraction of polygonal ferrite in the current research was maintained at ~50 to 55 pct for all experiments, to study the effect of the ferrite-grain refinement obtained through the deformation in the recrystallized austenite region on the mechanical properties of TRIP steel.

The samples were deformed to 0.25 and 0.50 strain in the recrystallized austenite region, while the strain in the nonrecrystallized austenite region was similar in both experiments (0.47). The microstructures obtained after these tests are shown in Figure 2. The microstructure after $\varepsilon_1 = 0.25$ and $\varepsilon_2 = 0.47$ consisted of 50 to 55 pct polygonal ferrite 30 to 35 pct carbide-free bainite, such as granular bainite and acicular ferrite, with retained austenite, retained austenite/martensite constituent, and martensite (Table II). Granular bainite is characterized by the absence of carbides, the presence of isolated regions of high-carbon austenite, and martensite between crystals of bainitic ferrite, which have a grain or plate morphology (Figure 3(a)).[16] The acicular ferrite structure is a bainitic structure with retained austenite and martensite between the bainitic ferrite laths (or lenticular plates) (Figure 3(b)).[17] The retained/martensite constituent appeared as coarse, blocky islands in the polygonal ferrite, between the polygonal ferrite grains, and in the bainitic ferrite laths or grains.

The average Vickers microhardness (VHN) of the bainitic phase was 284 VHN. This microstructure showed a good combination of ultimate tensile strength (~924 MPa) and total elongation (~49 pct, Table II) with yield strength (~537 MPa). This is likely to be due to the balance between the ductile ferrite matrix, hard martensite, and retained-austenite phase in the bainitic ferrite, in addition to the TRIP effect during tensile deformation.

Increasing the deformation in the recrystallized austenite region ($\varepsilon_1 = 0.5$) reduced the austenite grain size from ~45 μm (0.25 strain) to 35 μm and stimulated the formation of upper bainite with a small amount of a martensite/retained-austenite constituent (Figure 2(b)). The upper bainite consisted of parallel bainitic ferrite laths and carbides between these laths. The presence of the carbides in upper bainite reduced the volume fraction (<2 pct) of the retained austenite (Table I). The average microhardness of the upper-bainite phase was only 270 VHN.

The mechanical properties of the steel also deteriorated the ultimate tensile strength was ~ 810 MPa and the total elongation was ~ 30 pct (Table II), through changes in the bainite morphology and the reduction in the volume fraction of retained austenite. However, the yield strength increased to 610 MPa (Table II) with the change in the microstructure. Thus, an increase in strain in the recrystallized austenite region and a decrease in the austenite/ferrite grain size do not lead to an improvement of the mechanical properties of TRIP steel, as suggested by others.[10]

B. *Effect of Deformation in the Nonrecrystallized Austenite Region on the Microstructure and Mechanical Properties of TRIP Steel*

Austenite pancaking is achieved by deforming at temperatures below the nonrecrystallization temperature; this alters the substructure of the austenite prior to transformation.[18] For TRIP steels, the nature of the bainitic structure, which is affected by the transformation from nonrecrystallized austenite and, accordingly, the stability of retained austenite is crucial aspects to provide the TRIP effect.

The samples were deformed to strains of 0.47 and 1.2 in the nonrecrystallized region, while the strain in the recrystallized region was 0.25. The effect of the deformation in the nonrecrystallized austenite region on the microstructure is shown in Figure 2(c). After increasing the deformation in the nonrecrystallized region ($\varepsilon_2 = 1.2$), the pancaked austenite grain thickness decreased from ~45 μm (0.47 strain) to 25 μm. As a result, further refinement of the ferrite grain size was observed: from ~15 μm ($\varepsilon_2 = 0.47$) to 9 μm ($\varepsilon_2 = 1.2$) through the formation of additional nucleation sites inside the pancaked austenite grains.[19]

The microstructure after increasing the deformation in the nonrecrystallization region also contained polygonal ferrite, upper bainite, martensite, and 4 pct retained austenite (Figure 2(c)). The presence of carbides between the bainitic ferrite laths can dramatically reduce the carbon content in the retained austenite, leading to the transformation to martensite during quenching. This might be the reason why the volume fraction of retained austenite decreased after a 1.2 strain in the nonrecrystallization region. The average microhardness of the bainitic phase was ~250 VHN. The microhardness decreased because of the presence of upper bainite and a decrease in the retained-austenite content. However, in spite of a decrease in the volume fraction of retained austenite, the mechanical properties of the sample still exhibited a good combination of ultimate tensile strength (827 MPa), yield strength (555 MPa), and total elongation (35 pct) (Table II), because even a small amount of stable retained austenite can provide a TRIP effect, although significantly lower than in the case when granular bainite and acicular ferrite were present.

C. *Effect of Further Increase in the Deformation in the Recrystallized Austenite Region*

The resulting austenite grain thickness after a 0.25, 0.5, and 0.75 strain in the recrystallization region, with a strain in the nonrecrystallized region of 1.2, was ~25, 20, and

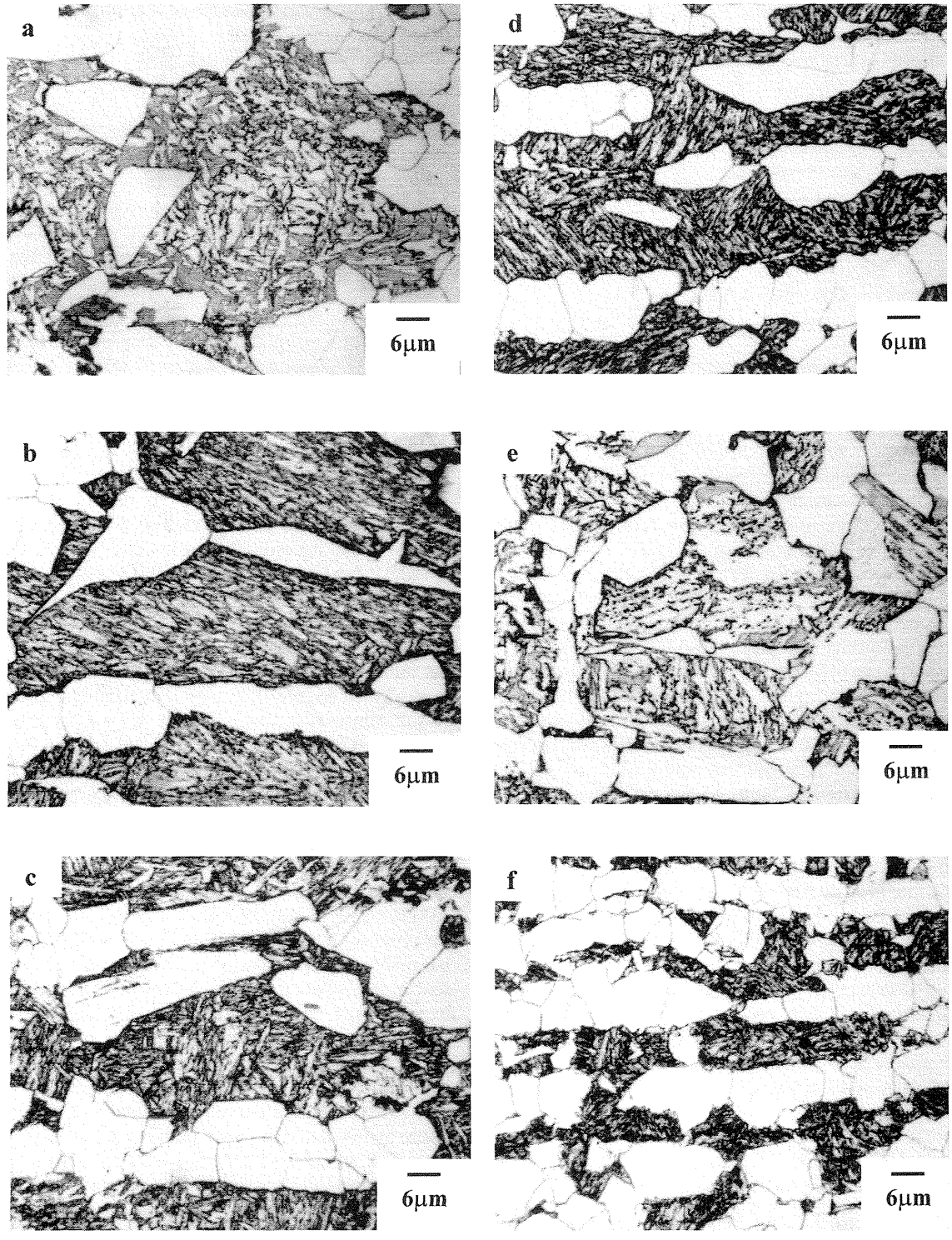

Fig. 2—Microstructures of the samples after (*a*) $\varepsilon_1 = 0.25$ and $\varepsilon_2 = 0.47$, (*b*) $\varepsilon_1 = 0.5$ and $\varepsilon_2 = 0.47$, (*c*) $\varepsilon_1 = 0.25$ and $\varepsilon_2 = 1.2$, (*d*) $\varepsilon_1 = 0.5$ and $\varepsilon_2 = 1.2$, (*e*) $\varepsilon_1 = 0.75$ and $\varepsilon_2 = 1.2$, (*f*) $\varepsilon_1 = 0.75$ and $\varepsilon_2 = 3.0$.

15 μm, respectively. The ferrite grain size also decreased from ~9 (0.25 strain) to 7.5 μm (0.5 strain) to 7 μm (0.75 strain). The microstructure after a strain of 0.5 in the recrystallization region also consisted of upper bainite (Figure 3(c)) and a small amount of retained austenite (less than 2 pct) in addition to the polygonal ferrite. The microstructure was similar to the microstructure after a 0.25 strain (Figures 2(c) and (d)). However, the further increase in the deformation in the recrystallized austenite region led to refinement of the bainitic packets (bainitic ferrite laths and carbides) compared with the 0.25 strain (Figure 4), which resulted in a higher average microhardness (287 VHN) compared with the 250 VHN obtained after $\varepsilon_1 = 0.25$ and $\varepsilon_2 = 1.2$. The formation of the upper bainite with fine

Table II. Effect of Deformation Schedule on the Microstructure and Mechanical Properties of TRIP Steel*

Schedules	$\varepsilon_1 = 0.25$ $\varepsilon_2 = 0.47$	$\varepsilon_1 = 0.5$ $\varepsilon_2 = 0.47$	$\varepsilon_1 = 0.25$ $\varepsilon_2 = 1.2$	$\varepsilon_1 = 0.5$ $\varepsilon_2 = 1.2$	$\varepsilon_1 = 0.75$ $\varepsilon_2 = 1.2$	$\varepsilon_1 = 0.75$ $\varepsilon_2 = 3.0$
Prior austenite grain width (μm)	45 ± 2.2	35 ± 2.7	25 ± 1.8	20 ± 2	15 ± 2.4	7 ± 1.9
Ferrite grain size (μm)	15 ± 1.2	10 ± 1.75	9 ± 2	7.5 ± 1.1	7 ± 1.5	5.5 ± 1.5
Morphology of the bainite	noncarbide granular bainite and acicular ferrite	upper bainite	upper bainite	upper bainite	granular bainite	refined bainite with carbides and retained austenite between bainitic ferrite
Volume fraction of retained austenite (pct)	0	<2	3 to 4	<2	6	4
Type of retained austenite	blocky islands and layers between BF and PF	ultrafine islands between BF	small islands between BF	ultrafine islands between BF	layers between BF	fine islands between BF
Volume fraction of martensite, (pct)	6	—	<2	—	9	8
Type of martensite	islands between PF and BF	—	small islands between bainite and PF	—	blocks between PF	coarse blocks between PF
Ultimate tensile strength (MPa)	924 ± 46	810 ± 40	827 ± 41	844 ± 42	890 ± 44	1000 ± 50
Total elongation (pct)	49 ± 2.45	30 ± 1.5	35 ± 1.75	33 ± 1.65	43 ± 2.2	32 ± 1.6
Yield strength (MPa)	537 ± 53	610 ± 61	555 ± 56	599 ± 60	510 ± 51	393 ± 39

*PF is polygonal ferrite, and BF is bainitic ferrite. The volume fractions of polygonal ferrite and bainite are similar for all experiments.

carbides between the bainitic ferrite laths reduced the chemical stability of the retained austenite and, consequently, the volume fraction of retained austenite.

Increasing the strain in the recrystallized austenite region to 0.75 with 1.2 strain in the nonrecrystallized austenite region promoted the formation of granular bainite with ~6 pct retained austenite and ~9 pct martensite, in addition to ~50 pct polygonal ferrite (Figure 2(e)). The microstructure was similar but more refined than that obtained after $\varepsilon_1 = 0.25$ and $\varepsilon_2 = 0.47$.

The average microhardness of the bainitic phase was 300 VHN. The retained austenite was in the form of the coarse blocks between the polygonal ferrite grains and layers between the bainitic ferrite laths. The increase in the volume fraction of the retained austenite was due to both the reduction in the polygonal ferrite grain size and the morphology of the carbide-free granular bainite structure.

The mechanical properties of the steel after strains of 0.25, 0.5, and 0.75 in the recrystallized austenite region are displayed in Table II. The ultimate tensile strength increased with decreasing austenite thickness and ferrite grain size, when the samples produced a similar bainitic structure, such as upper bainite in the case of $\varepsilon_1 = 0.25$ and $\varepsilon_1 = 0.5$. A similar tendency was observed for the yield strength (increasing from 555 to 599 MPa). A reduction of the ferrite grain size did not always lead to an increase in the elongation (Table II). It is proposed that the volume fraction and stability of the retained austenite play a more important role than the grain refinement in enhancing the elongation, particularly as grain refinement generally decreases ductility. The maximum ultimate tensile strength (883 MPa) and the total elongation (43 pct) was observed after a 0.75 strain (Table II), which produced the minimum ferrite grain size and maximum volume fraction of retained austenite and carbide-free bainitic structures, such as granular bainite and acicular ferrite. However, the relatively high and stable amount of retained austenite obtained in this carbide-free bainitic structure caused a decrease in the yield strength (510 MPa) (Table II).

D. *Effect of Severe Deformation in the NonRecrystallized Austenite Region*

The further increase in strain in the nonrecrystallized austenite region from 1.2 to 3 reduced the austenite grain thickness prior to transformation and the ferrite grain size: from ~15 to 7 μm and from ~7 to 6.5 μm, respectively. The microstructure after a strain of 3 in the nonrecrystallized region consisted of polygonal ferrite, bainite, ~8 pct martensite, and a small amount of retained austenite (Figure 2(f)). The bainitic structure consisted of heavily refined bainitic ferrite grains with small carbides and stable islands of retained austenite between the bainitic ferrite laths or

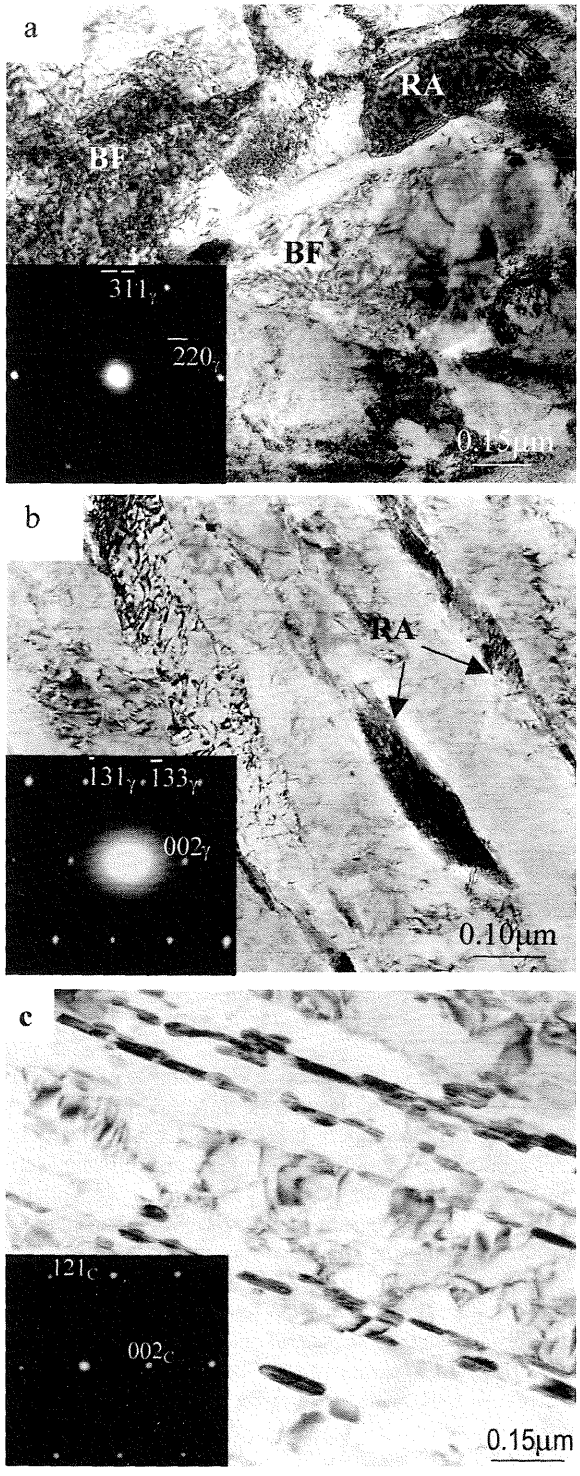

Fig. 3—TEM micrographs of the (*a*) granular bainite and (*b*) acicular ferrite after $\varepsilon_1 = 0.25$ and $\varepsilon_2 = 0.47$; and the upper bainite after (*c*) $\varepsilon_1 = 0.5$ and $\varepsilon_2 = 1.2$ (for (a), the zone axis is $[114]_\gamma$, for (b), the zone axis is $[310]_\gamma$, and for (c), the zone axis is $[\bar{2}10]_C$).

grains. It was observed that the heavy deformation changed the distribution of martensite. The majority of martensite was present in the form of large blocks between polygonal ferrite grains. This may be the reason for the decrease in yield strength to 393 MPa. The combination of the effect of grain refinement and distribution of phases resulted in an

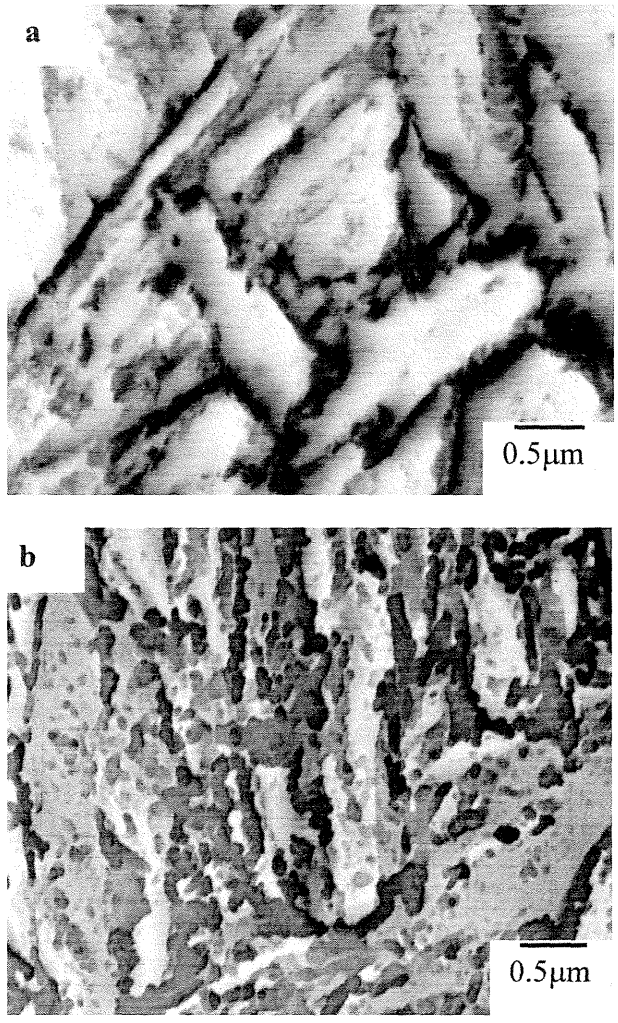

Fig. 4—SEM micrographs of the deformed samples: (*a*) and (*c*) $\varepsilon_1 = 0.25$ and $\varepsilon_2 = 1.2$; and (*b*) $\varepsilon_1 = 0.5$ and $\varepsilon_2 = 1.2$.

increase in the ultimate tensile strength to 1000 MPa and a decrease in the total elongation to 31 pct (Table II).

Thus, the mechanical properties of TRIP steels depend not only on the polygonal ferrite grain refinement and morphology of the bainitic phase, but also on the distribution of all phases present in the microstructure.

E. *The TEM Characterization of the Heavily Deformed Samples*

The TEM analysis revealed that the heavy deformation results in the formation of parallel bands of elongated bainitic ferrite subgrains with low-angle subgrain misorientations (Figure 5(a)). These subgrains showed the cell structure, *i.e.*, the dislocation-free region surrounded by the dislocation-cell walls (Figure 5(a)).[20,21] The average thickness of the subgrains after $\varepsilon_1 = 0.5$ and $\varepsilon_2 = 1.2$ was ~0.15 μm. Moreover, well-developed networks of interfacial dislocations were found within the bainitic ferrite laths. An increase in the deformation to $\varepsilon_1 = 0.75$ and $\varepsilon_2 = 3.0$ led to the formation of the equiaxed-shape bainitic ferrite subgrains free from dislocation within subgrains and a high density of dislocation tangles at the subgrain interfaces (Figure 5(b)).

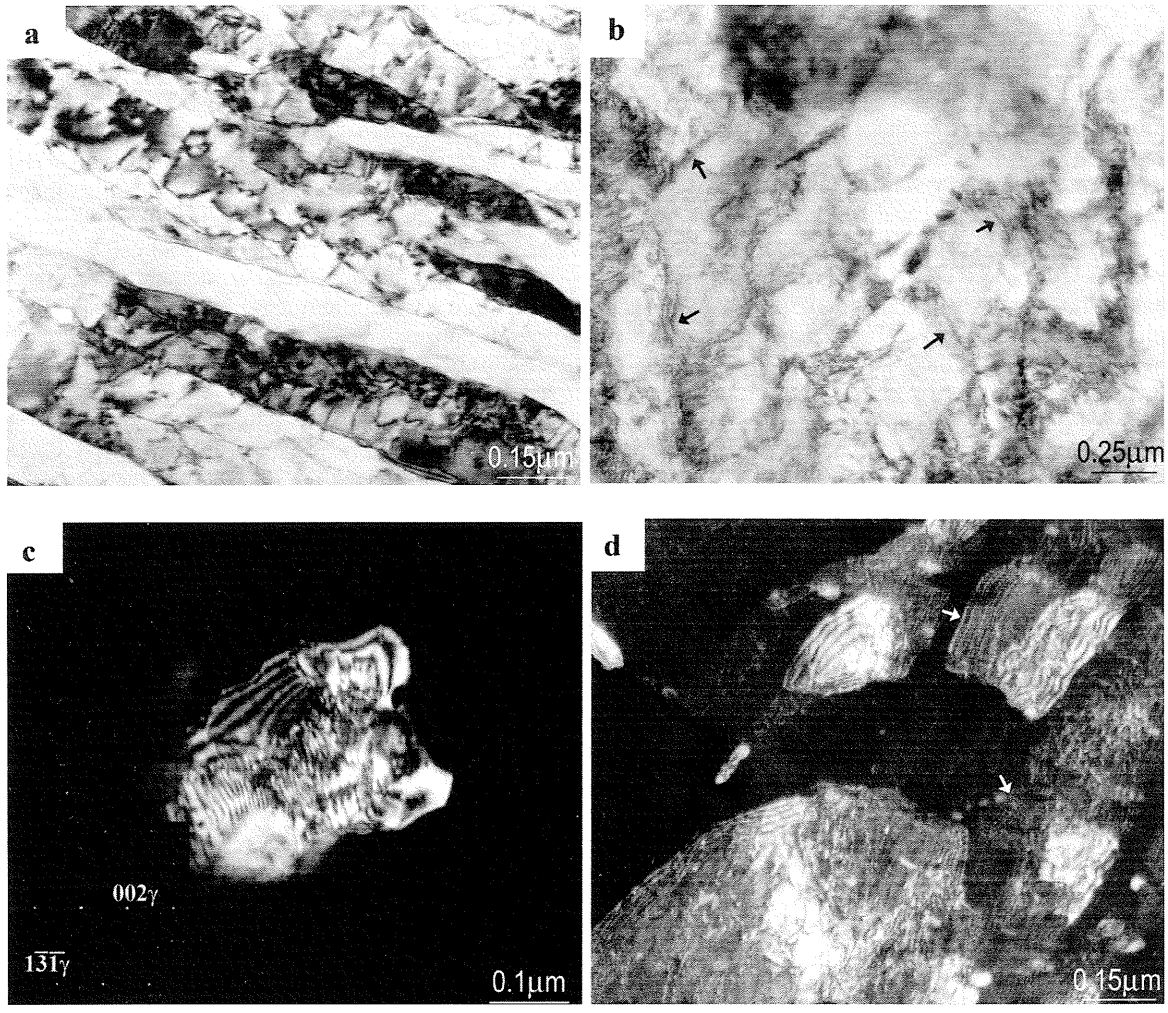

Fig. 5—TEM micrographs of the bainitic ferrite after (*a*) $\varepsilon_1 = 0.5$ and $\varepsilon_2 = 1.2$ and (*b*) $\varepsilon_1 = 0.75$ and $\varepsilon_2 = 3.0$; the retained austenite after $\varepsilon_1 = 0.75$ and $\varepsilon_2 = 1.2$ (*c*) and (*d*) dark-field images, and (c) from $(002)_\gamma$; the zone axis is $[310]_\gamma$). Arrows indicate the intergranular dislocations.

It was found that the retained austenite crystals present after deformation in the recrystallized and nonrecrystallized regions contained a high dislocation density inside the grains (Figure 5(c)) and a large number of interface dislocations (Figure 5(d)). This might contribute to an increase in the mechanical stability of the retained austenite.

The carbides were found between the bainitic ferrite laths in the upper bainite structure (Figure 3(c)). This may increase the ability of the bainitic ferrite lath boundaries to impede dislocation motion during straining, thereby confining slip within the laths and raising the contribution of the lath size of bainite to the flow stress.[22]

IV. DISCUSSION

A. *Effect of the Deformation Schedules on the Microstructural Evolution and Mechanical Properties of TRIP Steel*

The optimum amount of retained austenite is the critical aspect for TRIP steels. Based on the results of Kawano *et al.*,[10] the reduction of both the austenite and ferrite grain sizes should increase the quantity of retained austenite, because the volume fraction of retained austenite (V_{RA}) has been related to V_{PF}/d_{PF}, where V_{PF} is the volume fraction of polygonal ferrite, and d_{PF} is the grain diameter of polygonal ferrite. Hence, the increase in the degree of deformation in the recrystallized and nonrecrystallized austenite regions and the decrease in the ferrite grain size should increase the volume fraction of retained austenite and improve the total elongation for a similar amount of polygonal ferrite, for all experiments (~50 pct). Moreover, the amount of deformation could affect not only the polygonal ferrite grain size, but also the bainite morphology and retained-austenite stability through the prior-austenite grain refinement.[23]

The gradual increase in the amount of total strain (Table I) led to the gradual decrease in the resulting austenite thickness and polygonal ferrite grain size. Despite this, the volume fraction of retained austenite and the mechanical properties varied after different deformation tests.

The main difference in the microstructure after increasing the deformation in the recrystallized austenite region from 0.25 to 0.5 strain, at $\varepsilon_2 = 0.47$, was the formation of the carbide-containing upper bainite structure at 450 °C, instead of carbide-free granular bainite, as observed for

$\varepsilon_1 = 0.25$ and $\varepsilon_2 = 0.47$. This led to the sharp reduction in the retained austenite volume fraction in the microstructure (Table II). As was mentioned previously, an increase in the deformation in the recrystallized austenite region refined the austenite and ferrite grain sizes. However, the mechanical properties after this increase were deteriorated compared to $\varepsilon_1 = 0.25$ and $\varepsilon_2 = 0.47$ (Table II), due to the formation of the upper bainite structure. As was reported in an earlier publication,[15] the upper bainite structure should form at 500 °C to 550 °C for a TRIP steel with this composition. This change in the transformation kinetics could be explained by considering both the recrystallized and nonrecrystallized austenite conditions. Since the bainitic ferrite crystals nucleate at an austenite grain boundary, a reduction in the austenite grain size should lead to an increase in the rate of transformation because of the greater density of grain-boundary nucleation sites.[17] This refines the bainitic ferrite crystals. Moreover, since the bainitic ferrite inherits the dislocation density of the parent austenite,[17] the decrease in the recrystallized austenite grain size and the deformation of these recrystallized grains in the nonrecrystallized austenite region lead to the increase in the dislocation density of the bainitic ferrite and in the total grain boundary area, which results in a larger number of barriers to the dislocation motion.[24] It was suggested that the combined effect of the bainitic ferrite refinement and the dislocation density of the parent austenite increase the rate of carbon diffusion and the number of diffusion paths for carbon (grain boundary diffusion and pipe diffusion) that accelerate the carbide formation and, as a result, upper bainite was formed in sample after $\varepsilon_1 = 0.5$ and $\varepsilon_2 = 0.47$ (Figure 2(b)). This decreases the retained austenite content in the microstructure and affects the mechanical properties of steel.

The volume fraction of bainite after $\varepsilon_1 = 0.5$ and $\varepsilon_2 = 0.47$ and holding at 450 °C for 600 seconds was similar to that observed after $\varepsilon_1 = 0.25$ and $\varepsilon_2 = 0.47$. According to Shipway and Bhadeshia, deformed austenite transforms to a smaller quantity of bainite than undeformed austenite.[25] However, when the strain increases beyond a certain value, the corresponding increase in nucleation-site density leads to a recovery in the attainable fraction of bainite, and this may be similar to that of undeformed or slightly deformed austenite.[25] The conclusion from this result could be that the optimal level of deformation has been already obtained during these experiments.

The quality of retained austenite depends on the mechanical and chemical stability. The refinement of the bainite packets obtained by increasing the density of nucleation sites within pancaked austenite grains should enhance the retained austenite stability by decreasing the retained austenite size (the smaller retained austenite is more stable), which typically increases the carbon content in the retained austenite lattice.

Increasing the deformation in the nonrecrystallized austenite region from 0.47 to 1.2 strain at $\varepsilon_1 = 0.25$ also led to the formation of the upper bainite (Figure 2(c)), which is most likely because the bainite transformation was further affected by the increased deformation debris in the nonrecrystallized austenite.[11] However, it was observed that the bainitic structure was more refined than that after $\varepsilon_1 = 0.25$ and $\varepsilon_2 = 0.47$.

The further increase in the total deformation from increasing the nonrecrystallized deformation to a 1.2 strain, at a 0.5 strain in the recrystallized austenite region, did not change the type of the bainite. The microstructure still contained upper bainite as a major bainitic phase. However, the combination of $\varepsilon_1 = 0.5$ and $\varepsilon_2 = 1.2$ significantly changed the morphology of bainitic ferrite by (1) increasing the misorientations between the bainitic ferrite laths and (2) significantly refining the bainitic ferrite laths (Figure 4). It was suggested that a heavy deformation enhances the nucleation of bainitic ferrite within nonrecrystallized austenite grains, which refines the bainitic ferrite packets.

Moreover, the significant refinement of the bainitic structure after $\varepsilon_1 = 0.5$ and $\varepsilon_2 = 1.2$ can also be explained by the formation of the dislocation-cell structures (or subgrain structure) in the heavily deformed austenite (Figure 5(a)). The bainitic ferrite laths stop their growth at the cell-structure boundaries, which then reduces their length.[11] This could explain the bainitic structure refinement obtained after this deformation test. On the contrary, in the case of $\varepsilon_1 = 0.25$ and $\varepsilon_2 = 1.2$, the dislocation density, which forms the dislocation-cell structure, was low, and the bainitic ferrite laths, which nucleate on the austenite grain boundaries, grow linearly, and stop their growth only on the opposite austenite grain boundaries (Figure 3(c)).[11]

The carbide-free granular bainite (similar to that obtained after $\varepsilon_1 = 0.25$ and $\varepsilon_2 = 0.47$) was formed only after increasing the amount of deformation in the recrystallized austenite region up to 0.75 strain at 1.2 strain in the nonrecrystallized austenite region (Figure 2(e)). The formation of this bainitic structure led to the increase in the volume fraction of retained austenite to 6 pct, present in the form of layers between the bainitic ferrite laths. It appears that the retained austenite with this particular morphology within the carbide-free granular bainite increased the elongation of the sample, while the refinement of the polygonal ferrite and bainite increased the ultimate tensile strength of steel compared to the samples with the upper bainite structure (Table II). Thus, instead of the upper bainite structure, granular bainite, which is a transformation product at a lower isothermal temperature,[15] was obtained at this amount of deformation. This effect can occur when the strain accumulates in the austenite and reaches a certain critical value. A reduction in the austenite grain size reduces the total volume transformed per nucleus and retards the overall reaction rate.[17] When the growth of the bainitic ferrite laths by a shear mechanism is limited by their volume fraction, the austenite remaining between the bainitic ferrite laths could be mechanically stabilized. This could retard the formation of the carbides.[17] So, the increase in the amount of total deformation to the critical level could change the bainite transformation kinetics. In the current research, this level was obtained at $\varepsilon_1 = 0.75$ and $\varepsilon_2 = 1.2$, which leads to the formation of granular bainite (Figure 2(e)). In addition to the effect of the deformation in the recrystallized austenite region, the effect of the nonrecrystallized austenite condition on the transformation kinetics should be considered. Displacive transformation occurs by the advance of glissile interfaces, which can be rendered sessile, when they encounter dislocation debris in the austenite.[17]

So, with increasing the dislocation density in the nonrecrystallized austenite, the bainitic transformation is retarded regardless of the increase in the number density of nucleation sites. This also might lead to the formation of the carbide-free bainite.

A further increase in the amount of deformation ($\varepsilon_1 = 0.75$ and $\varepsilon_2 = 3.0$) led to the unexpected effects. The main feature of the heavily deformed ($\varepsilon_1 = 0.75$ and $\varepsilon_2 = 3.0$) microstructure was the formation of small and stable islands of retained austenite and the formation of the high quantity of martensite between the polygonal ferrite grains and at the polygonal ferrite/bainite interface (Figure 2(f)). The heavy deformation in the recrystallized and nonrecrystallized austenite regions heavily refined the bainitic structure, which led to a decrease in the volume fraction and size of the retained austenite within the bainite. This could increase the carbon concentration of the retained austenite and, subsequently, its stability. This retained austenite trapped within the refined bainitic structure did not transform to martensite during the deformation and did not provide the TRIP effect; even the presence of a small amount of the carbides in the bainitic structure did not diminish this effect. This reduced the elongation of the sample (Table II). The high volume fraction of martensite in a soft ferrite matrix could be explained by the distribution of retained austenite prior to quenching. The polygonal ferrite was less affected by the amount of deformation than was the bainite. The nucleation of bainite leads to an additional invariant plane-strain shape deformation with a large shear component, which is similar to that of martensite.[25] This could decrease the ability of the retained austenite to be located between bainitic ferrite, and, as a result, most of the austenite remained between the polygonal ferrite grains and at the polygonal ferrite/bainite interface. On the other hand, the stability of retained austenite depends on the carbon content in the remaining austenite lattice. The enrichment of the retained austenite by carbon occurs during the polygonal ferrite and bainite transformations. Coarse blocks of austenite between polygonal ferrite are less enriched by carbon and are less stable during quenching. It is proposed that this was the reason why the microstructure contained the higher volume fraction of martensite between the polygonal ferrite. The high volume fraction of martensite increased the ultimate tensile strength of the sample (Table II). Hence, the formation of the heavily refined polygonal ferrite and bainitic structure might lead to the deterioration of the mechanical properties of the TRIP steel due to the distribution and morphological features of martensite and retained austenite within the microstructure.

B. *Microstructure-Property Relationship*

The microstructure of the TRIP steel could be characterized in terms of a number of morphological features, such as the size and morphology of the bainitic packets, the volume fraction and distribution of retained austenite and martensite within the microstructure, and the volume fraction and morphology of polygonal ferrite. These features should be related to the mechanical properties of TRIP steel.

As mentioned previously, the volume fraction of polygonal ferrite was similar for all experiments (~50 pct). The contribution of polygonal ferrite to the mechanical properties depends on the grain size (Table II). A decrease in the grain size generally leads to an increase in the ultimate tensile strength and the yield strength through the Hall–Petch relationship:

$$\sigma_y = K + k_y d^{-1/2} \quad [3]$$

where σ_y is the lower yield stress, K is the material constant, k_y is the strengthening coefficient, and d is the ferrite grain size.[22] A sharp yield point was not observed during all tensile tests.

However, it was found that the yield strength of the TRIP steel was not only a function of the grain size. The ferrite grain size does contribute to the yield strength, but there are other factors affecting the yield strength, as polygonal ferrite is only one component of the microstructure. According to Edmonds and Cochrane,[22] it is possible to account for the strength of the bainitic structure in terms of four major contributions:

1. a term relating to slip-band length, which includes both colony (packet) and lath size;
2. a term due to the dislocation substructure within the laths;
3. a term including solid-solution hardening from substitutional elements, such as Si, Mn, Ni, *etc.*, but additional interstitial hardening from C and N;
4. a term which arises from the dispersion-hardening effect of the carbide particles.

Furthermore, the morphology and distribution of the retained austenite and martensite play an important role in the structure-property relationship.

The microstructures (Figures 2) resulting from various deformation tests have been described previously. The presence of 10 pct retained austenite in the carbide-free bainitic structure after $\varepsilon_1 = 0.25$ and $\varepsilon_2 = 0.47$ led to low yield stress (537 MPa) with a good combination of ultimate tensile strength and total elongation (Table II). These mechanical properties reflect the changes in the microstructure during straining. The transformation of metastable retained austenite to martensite during deformation leads to the improvement of elongation and the creation of new dislocations, which leads to the reduction in the yield strength.

The formation of the upper-bainite structure with coarse carbides between parallel bainitic ferrite laths (Figure 2(b)), after a 0.5 strain in the recrystallized austenite region and at $\varepsilon_2 = 0.47$, led to a reduction in the volume fraction of retained austenite (<2) and an increase in the yield strength (Table II). Carbides influence the ability of the lath boundaries to impede dislocation motion, thereby confining slip to within the laths and increasing the lath-size contribution to the flow stress.[22]

As mentioned earlier, the upper-bainite structure was also formed by increasing the strain in the nonrecrystallized austenite region from 0.47 to 1.2 strain at $\varepsilon_1 = 0.25$. The yield strength increased compared with the lower deformation conditions ($\varepsilon_1 = 0.25$ and $\varepsilon_2 = 0.47$), due to the presence of coarse carbides in the upper-bainite structure. However, the yield strength was lower than in the case of $\varepsilon_1 = 0.5$ and $\varepsilon_2 = 0.47$. This reduction depends on the distribution of retained austenite and martensite before straining. Retained austenite appeared as small, stable islands, uniformly distributed between the bainitic ferrite laths. These fine crystals of retained austenite could contribute to the reduction in the yield strength. On the other hand, the blocks of martensite formed between the polygonal ferrite and bainite also enhance this reduction by the generation of the new mobile dislocations in the parent ferrite matrix prior to straining. The movement of these unobstructed dislocations results in the yield-strength reduction, as commonly observed in dual-phase steel.[26]

The microstructure after $\varepsilon_1 = 0.5$ and $\varepsilon_2 = 1.2$ was similar to the microstructure after $\varepsilon_1 = 0.25$ and $\varepsilon_2 = 1.2$ (Figure 2(d)). However, the refinement of the polygonal ferrite and bainitic structure obtained after this experiment led to an increase in the yield strength (Table II). This may be due to the refinement of the bainitic packets, which hinders the dislocation motion. The strength of bainitic steel can be better described in terms of the Langford–Cohen model for substructural strengthening, $\sigma_y \sim (L)^{-1}$, where L is the average transverse bainitic lath width.[27] In addition, bainitic ferrite makes a significant contribution to strength in its own right, due to its carbon supersaturation and high dislocation density. Furthermore, the bainitic structure contains a variety of obstacles to dislocation motion, (solute atoms, precipitates of different size, and boundaries), each with a different ability to impede plastic deformation. Hence, the reduction of grain size only led to an increase in the yield strength when the contribution to the mechanical properties of the morphology of different phases in the microstructure was negligible.

The formation of the carbide-free granular bainite structure with 6 pct retained austenite after $\varepsilon_1 = 0.75$ and $\varepsilon_2 = 1.2$ led to the decrease in the yield strength to 510 MPa. This result demonstrates an almost similar yield strength value (537 MPa) to that obtained after $\varepsilon_1 = 0.25$ and $\varepsilon_2 = 0.47$ with a similar microstructure. Hence, the yield strength reduction was due to the combined effect of the grain refinement and the morphology of the bainite.

As mentioned previously, the heavy deformation ($\varepsilon_1 = 0.75$ and $\varepsilon_2 = 3.0$) significantly affected the distribution of the retained austenite before quenching (Figure 2(f)) by (1) increasing the volume fraction of less-stable austenite between the polygonal ferrite grains and at the polygonal ferrite/bainite interface, which transformed to martensite during quenching and, (2) on the other hand, decreasing the volume fraction and size of the stable retained austenite within the bainitic structure. Moreover, the yield strength decreased to 393 MPa. The stable retained austenite within the bainitic structure did not affect the yield strength. In this case, the volume fraction, morphology (coarse blocks), and location of martensite within the soft ferrite matrix were more significant in determining the structure-property dependence. The distribution of different phases within the microstructure is important, because when a large fraction of a phase harder than bainite, such as retained austenite or martensite, is included in a soft matrix, plastic deformation at first occurs in the softer phase. On the other hand, the hard phase only begins to deform when the softer phase has strain hardened sufficiently to transfer load. The hard martensite phase under straining can stimulate the formation of new mobile dislocations in a soft ferrite matrix and, by means of this, decrease the yield strength.[28] Furthermore, the martensite was not uniformly distributed within the ferrite, so giving rise to a gradual deviation from elastic deformation. Hence, it is proposed that all these features decrease the yield strength.

V. CONCLUSIONS

The effect of the heavy deformation in the recrystallized and nonrecrystallized austenite region on the transformation kinetics and mechanical properties of TRIP steel was studied. The findings were as follows.

1. Ferrite grain refinement does not always lead to an increase in the volume fraction of retained austenite, because of the role of the bainite morphology.
2. The contribution of the grain refinement to the mechanical properties of TRIP steel is less than the effect of the bainite morphology and the stability of retained austenite.
3. The deformation schedule and amount of strain in the recrystallized and nonrecrystallized austenite regions affect the bainite transformation kinetics and morphology of bainite. The most superior combination of the ultimate tensile strength and total elongation was found after $\varepsilon_1 = 0.25$ and $\varepsilon_2 = 0.47$ and $\varepsilon_1 = 0.75$ and $\varepsilon_2 = 1.2$ in the samples with granular bainite and a maximum amount of the retained austenite.
4. Severe deformation affects the distribution of retained austenite and martensite present in the microstructure, which might influence the retained austenite stability.
5. The decrease in the ferrite grain size does not always lead to the increase in the yield strength of TRIP steel. The yield strength strongly depends on the morphology of the bainite, the distribution of the retained austenite and martensite within the microstructure, and phase interactions during testing.

ACKNOWLEDGMENTS

The authors express their gratitude to BHP Research for providing experimental steels. They also acknowledge the assistance in hot torsion testing from Mr. J. Whale. IBT is grateful to the Deakin University for provision of a scholarship.

REFERENCES

1. T. Gladman: *The Physical Metallurgy of Microalloyed Steels*, The Institute of Materials, Cambridge, United Kingdom, 1997, pp. 1-17.
2. V.F. Zackay, E.R. Parker, D. Fahr, and R. Busch: *Trans. ASM*, 1967, vol. 60, pp. 252-59.
3. W.W. Gerberich, P.L. Hemmings, M.D. Merz, and V.F. Zackay: *Trans. Techn. Notes*, 1968, vol. 61, pp. 843-47.
4. S.K. Liu and J. Zhang: *Metall. Trans. A*, 1990, vol. 21A, pp. 1517-25.
5. O. Matsumura, Y. Sakuma, Y. Ishii, and J. Zhao: *Iron Steel Inst. Jpn. Int.*, 1992, vol. 32 (10), pp. 1110-16.
6. Y. Sakuma, O. Matsumura, and H. Takechi: *Metall. Trans. A*, 1991, vol. 22A, pp. 489-98.
7. L.C. Chang and H.K.D.H. Bhadeshia: *Mater. Sci. Technol.*, 1995, vol. 11, pp. 874-81.
8. D.Q. Bai, A. DiChiro, and S. Yue: *Mater. Sci. Forum*, 1998, vols. 284–286, pp. 253-60.
9. F.B. Pickering: *Physical Metallurgy and Design of Steels*, Applied Science Publishers Ltd., Barking, Essex, United Kingdom, 1978, p. 64.
10. O. Kawano, J. Wakita, K. Esaka, and H. Abe: *Iron Steel Inst. Jpn. Int.*, 1996, vol. 82, pp. 232-44.
11. K. Fujiwara and S. Okaguchi: *Mater. Sci. Forum*, 1998, vols. 284–286, pp. 271-78.
12. P.D. Hodgson, D.C. Collison, and B. Perret: *Proc. 7th Int. Symp. on Physical Simulation of Casting, Hot Rolling and Welding*, 1997, Dynamic Systems Inc., Japan, vols. 21-23, pp. 219-29.
13. A. Zarei-Hanzaki: Ph.D. Thesis, McGill University, Montreal, 1994, pp. 44-45.
14. G.E. Lucas, J.W. Sheckherd, and G.R. Obette: *Shear Punch and Microhardness Tests for Strength and Ductility Measurements*, ASTM STP 888, ASTM, Philadelphia, PA, 1986, pp. 112-40.
15. I.B. Timokhina, E.V. Pereloma, and P.D. Hodgson: *Mater. Sci. Technol*, 2001, vol. 17, pp. 135-40.
16. S.W. Thompson, D.J. Colvin, and G. Krauss: *Metall. Trans. A*, 1990, vol. 21A, pp. 1493-507.

17. H.K.D.H. Bhadeshia: *Bainite in Steel, Transformation, Microstructure and Properties*, 2nd ed., The Institute of Materials, Cambridge University Press, Cambridge, United Kingdom, 2001, pp. 201-24 and 237.
18. S. Yue, A. DiChiro, and A. Zarei-Hanzaki: *JOM*, 1997, pp. 59-61.
19. R. Bengochea, B. Lopez, and I. Gutierrez: *Metall. Mater. Trans. A*, 1998, vol. 29A, pp. 417-26.
20. D.A. Hughes and N. Hansen: *Acta Mater.*, 1997, vol. 45 (9), pp. 3871-86.
21. N. Hansen: *Scripta Metall.*, 1992, vol. 27, pp. 1447-52.
22. D.V. Edmonds and R.C. Cochrane: *Metall. Trans. A*, 1990, vol. 21 A, pp. 1527-39.
23. K. Fujiwara and S. Okaguchi: *Mater. Sci. Forum*, 1998, vols. 284-286, pp. 271-78.
24. A.J. DeArdo: *Thermomechanical Processing of Steels*, 2000, IOM, London, vol. 1, pp. 309-21.
25. P.H. Shipway and H.K.D.H. Bhadeshia: *Mater. Sci. Technol.*, 1995, vol. 11, pp. 1116-28.
26. F. Hassani and S. Yue: *41st MWSP Conf. Proc.*, ISS, Warrendale, PA, 1999, vol. XXXVII, pp. 493-98.
27. G. Langford and M. Cohen: *Trans. ASM*, 1969, vol. 62, pp. 623-38.
28. T. Kvackaj and I. Mamuzic: *Iron Steel Inst. Jpn. Int.*, 1998, vol. 38 (11), pp. 1270-76.